



Cite this: DOI: 10.1039/d3nj01174g

Received 12th March 2023,  
Accepted 29th April 2023

DOI: 10.1039/d3nj01174g

rsc.li/njc

# A deep learning framework for predictions of excited state properties of light emissive molecules†

Zheng Tan,<sup>a</sup> Yan Li,<sup>a</sup> Ziyang Zhang,<sup>c</sup> Thomas Penfold,<sup>d</sup> Weimei Shi,<sup>a</sup> Shiqing Yang<sup>a</sup> and Wanli Zhang<sup>b</sup>

**We have implemented a deep learning protocol to forecast the excited state properties for thermally activated delayed fluorescence (TADF) molecules with satisfactory accuracies being achieved. In particular, for the oscillator strengths, predictive precisions have been significantly improved when the torsional profile of the dataset is enriched.**

Thermally activated delayed fluorescence (TADF) materials, known as the third generation of luminescent materials, have been extensively studied in the past decade due to their huge potential in making high efficiency organic light-emitting diode (OLED) devices.<sup>1–6</sup> To simply demonstrate its operating mechanism, upon electric excitation, TADF molecules can get thermally activated to trigger efficient reverse intersystem crossing (rISC) owing to the small singlet–triplet energy gap. As illustrated in Fig. 1, the triplet exciton can get up-converted into a singlet exciton through the rISC, leading to delayed fluorescence with a theoretical internal quantum efficiency approaching 100%. Compared to the conventional fluorescent and phosphorescent emitters, TADF materials have the advantages of larger material space, low fabrication cost without the use of heavy atoms, and more stable blue light emission.

The design of TADF molecules is however challenging, since it requires the optimization of two opposing quantities, *i.e.*, the oscillator strength  $f$  and the first singlet–triplet splitting  $\Delta E_{ST}$ . An efficient emission in TADF requires  $f$  to be maximized and  $\Delta E_{ST}$  to be minimized, which would correspond to increasing

and reducing the frontier orbital overlap. Currently, most of the TADF design is based on the donor–acceptor architecture,<sup>8–10</sup> within which the D–A dihedral twisting is properly adjusted to realize the separation of the frontier orbitals (*i.e.*, HOMO and LUMO), and a non-trivial oscillator strength simultaneously.

The rational design of TADF materials requires the singlet–triplet gap and the oscillator strength to be accurately estimated. It is known that time-dependent density functional theory (TDDFT) can have reasonable accuracy in describing the excited state properties,<sup>12</sup> and thus it has been extensively used in high throughput screenings for the exploration of the TADF search space.<sup>11</sup> However, high throughput calculation can suffer from a disreputable computational cost due to the large number of molecules involved. With the advent of machine learning (ML), materials discovery has come into a big data driven paradigm, which is expected to significantly shorten the material research and development cycle. Particularly for TADF molecules, deep neural network (DNN) has been employed to predict the photo-physical properties including the TADF luminescence rate

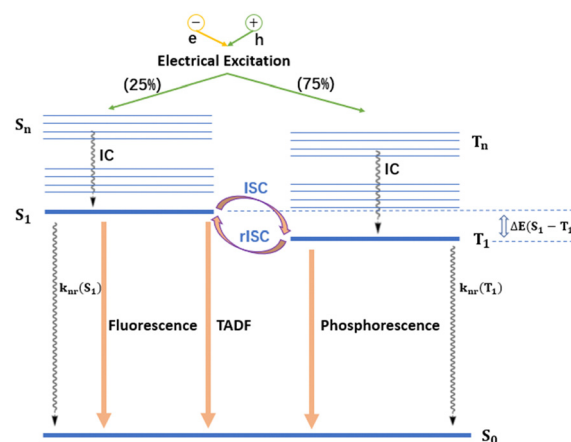


Fig. 1 Schematic diagram for the luminescence process of thermally activated delayed fluorescence molecules.

<sup>a</sup> Chengdu Polytechnic, 83 Tianyi Street, Chengdu, Sichuan, 610000, P. R. China.  
E-mail: zhengtian1983@hotmail.com

<sup>b</sup> State Key Laboratory of Electronic Thin Films and Integrated Devices, University of Electronic Science and Technology of China, Chengdu, 611731, P. R. China

<sup>c</sup> Guangzhou Yinfa Information Technology, 2 Ruyi Road, Panyu District, Guangzhou, 511431, P. R. China

<sup>d</sup> Chemistry-School of Natural and Environmental Sciences, Newcastle University, Newcastle Upon Tyne, NE1 7RU, UK

† Electronic supplementary information (ESI) available. See DOI: <https://doi.org/10.1039/d3nj01174g>

constant,<sup>12</sup> singlet and triplet excitation energies and oscillator strengths.<sup>7</sup> It is observed that, for the transition energies and the corresponding rate constant, DNN can make high quality predictions with an accuracy comparable to that of TDDFT calculations. Nevertheless, for the oscillator strengths, the prediction is less accurate, especially for the higher excited states. The reason has been tentatively attributed to the fact that the 2-dimensional fingerprint employed in DNN cannot figure out the 3-dimensional twisting information, which is critical for the estimation of oscillator strength.<sup>7</sup> Similar issues have also been encountered in Lu *et al.*<sup>13</sup> and Kang *et al.*'s<sup>14</sup> work, in which it is claimed that the ML should be used with caution for the prediction of transition dipole moment.

In order to provide a comprehensive scenario for the ML-assisted simulation of TADF materials, this article investigates the predictive performances of five state-of-the-art deep learning methods on the electronic transition properties that are directly related to the optoelectronic applications of TADF. Deep neural network (DNN), graph convolutional network (GCN), recurrent neural network (RNN), message passing neural network (MP) and SchNet models are employed to learn the 1-dimensional, 2-dimensional and 3-dimensional representations of molecules for the fitting of excited state energies and oscillator strengths. A TADF dataset (containing 13 594 samples) with molecules being of donor-acceptor structure (where high throughput TDDFT calculations are implemented to label the dataset, as described in the supplementary material) is used for the model training, validation and testing. Prediction accuracies are compared between different models, where SchNet is found to outperform the others. The cut-off effect of the 3-dimensional models (including SchNet and message passing) is also examined in an attempt to evaluate how the long-range interactions can influence the electronic properties. Moreover, we have built a conformer database based on the original D-A molecules, by extending the torsional profiles of TADF so that more twisting information can be involved. It is observed that the predictive performances for the oscillator strengths can be significantly improved when models are applied on the conformer dataset.

Detailed descriptions regarding the TADF database construction and the deep learning methodologies are given in the supplementary material.

Fig. 2 shows the prediction performances of the five deep learning models for the excited state properties of TADF molecules. Statistical estimates including the  $R^2$ , root mean squared error (RMSE) and mean absolute error (MAE) are evaluated. The  $R^2$  of the singlet and triplet energies is roughly in the range of 0.7–0.9 for different models, demonstrating the satisfactory performances for the transition energy predictions when deep learning methods are applied. The  $R^2$  of the first oscillator strength is still above 0.7, which is acceptable, while that for the higher excited states is significantly decreased. The observation is consistent with the works in Lu *et al.*<sup>13</sup> and Tan *et al.*<sup>7</sup> where enlarged uncertainties are encountered when deep learning is employed to predict the transition dipole. For the singlet–triplet energy splitting, all models achieve a  $R^2$  above 0.85, implying the robustness of the models in simulating the delayed fluorescence properties.

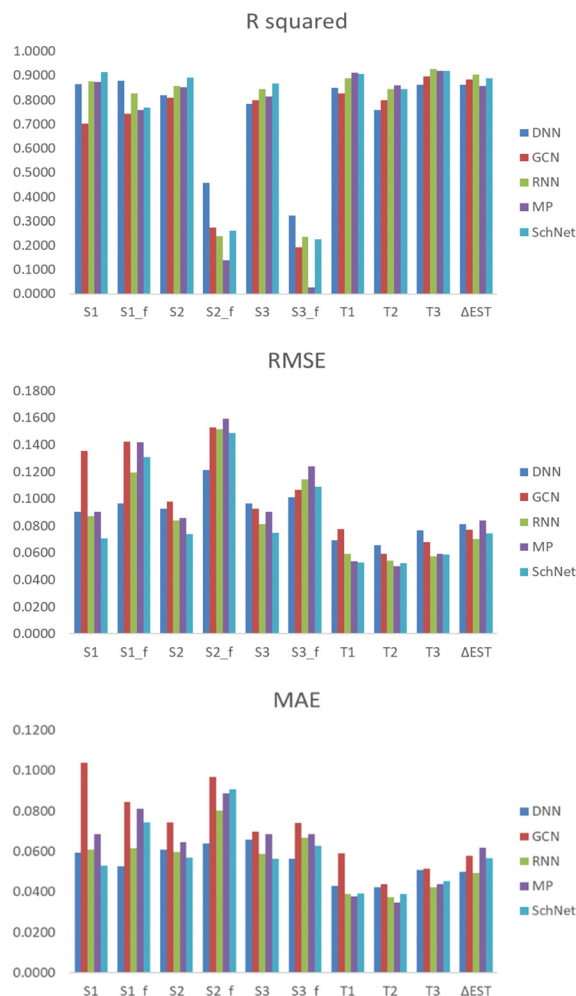


Fig. 2 Statistical estimates of prediction accuracies for excited state properties in the test set.  $S_1$ ,  $S_2$ ,  $S_3$ ,  $T_1$ ,  $T_2$ , and  $T_3$  represent the first three singlet and triplet excited state energies, while  $f$  denotes the corresponding oscillator strength, and  $\Delta E_{ST}$  the first singlet–triplet gap. Note that for RMSE and MAE, the energies are in the unit of eV, while  $f$  is dimensionless. For the MP and SchNet models, the cut-off radius is set to be 5 and 20 Å, respectively.

To compare performances between models, DNN, RNN and SchNet give rise to relatively better forecasting accuracies on average (as illustrated in Table 1) than GCN and MP. It is interesting that the 3-dimensional model (represented by SchNet) does not necessarily outperform the 1-dimensional (typified by RNN) and 2-dimensional (typified by DNN) models, even though it can involve more geometrical information of molecules. Notice that RNN utilizes the 1-dimensional character string as input, DNN employs the circular fingerprint to characterize the 2-dimensional molecular topology, while SchNet uses molecular composition and atomic positions for subsequent convolutional operations. The comparable performances delivered from these three neural networks using different input dimensions demonstrate the diversity of model designs that can be suitable to capture the excited-state properties.

Specifically for each model, DNN has the best prediction accuracies on the three singlet oscillator strengths. GCN has

**Table 1** Test set average performances of deep learning models for excited state properties. For RMSE and MAE, simple averaging is performed over the ten targets even though the units of energies and oscillator strengths are different. Similar to Fig. 2, the cut-off radius of the MP and SchNet models is set to be 5 and 20 Å, respectively

Test set average performance	$R^2$	RMSE	MAE
DNN	0.7466	0.0892	0.0546
GCN	0.6925	0.1010	0.0716
RNN	0.7451	0.0880	0.0556
MP	0.7018	0.0939	0.0619
SchNet	0.7489	0.0847	0.0575

moderate performance almost on all predicting targets, indicating a possible insufficiency of the molecular 2-dimensional graph in predicting the excited state properties (note that the result is in significant contrast with the ground state property predictions where GCN usually gives the best precision<sup>15</sup>). RNN performs good enough for most of the properties although the model only takes the SMILES string as input, which does not involve any structural characteristics. MP works well in excited state energy predictions, especially for those triplet state energies where  $R^2$  above 0.9 is achieved. It however performs poorly for the oscillator strengths (except for the first excited state), with  $R^2$  of 0.03 for  $S_{3-f}$  being visualized. The result demonstrates that the 3-body-correlation based neural network may not be suitable to describe the higher order transition dipole. Regarding SchNet, the best average performance in the test set is observed compared to other models (Table 1). The MAE of the transition energies (including both singlet and triplet) from SchNet is given in the range of 0.03–0.05 eV, which is comparable with the predictive error of excited state energies for organic semiconductors.<sup>13</sup> The fact that SchNet can deliver good enough performance in both the ground state<sup>16</sup> and excited state (in this research) properties indicates that the model may capture the main features in quantum many-body physics to resolve the electronic structure.

The cut-off effect of the 3-dimensional models (including MP and SchNet) is also examined, with no systematic correlation being found between the prediction accuracy and the cut-off radius. Detailed analysis is provided in the supplementary material.

Considering the complexity in the prediction of oscillator strengths, we have developed a conformer dataset based on the original D–A molecules by extending the molecular torsional profiles, so that more twisting information (which is important for the estimation of oscillator strengths) can be involved in the training input to elevate the model robustness. The conformer set is built through a stochastic search algorithm (experimental-torsion basic knowledge distance geometry<sup>17</sup>) by randomly generating the molecular conformations that satisfy various geometric constraints including lower/upper bounds on interatomic distances and torsional-angle preferences (using the module called ETKDGV3 as implemented in RDKit). As illustrated in Fig. 3, the initial conformations are produced by twisting the molecular fragments across the rotatable bond according to the experimental torsional-angle preferences. As the rotatable bond

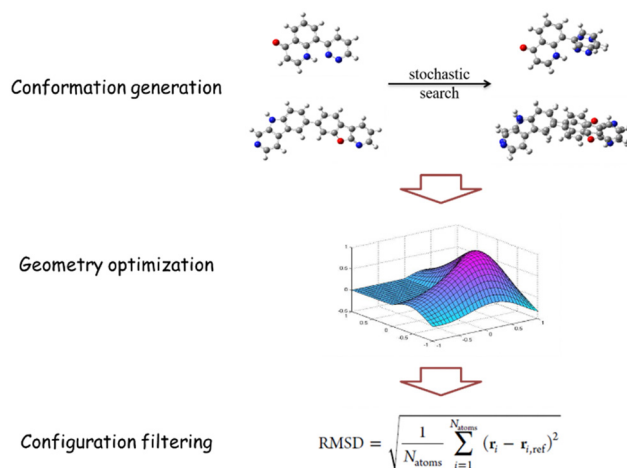


**Fig. 3** Flowchart for the conformer set development, including conformation generation via the stochastic search algorithm, force field geometry optimization and configuration filtering based on the RMSD (root-mean-square deviation) cut-off. Note that RMSD is defined as the root-mean-square displacement of atomic positions between a generated conformer and the reference structure. The reference denotes the minimal energy conformation within the generated conformer group.

is located between the donor–acceptor moiety for most TADF molecules, the action essentially creates a group of twisted D–A conformers. A geometry optimization is then performed on the generated conformations using the MMFF94 force field<sup>18</sup> to settle the conformers onto the energy local minima. A configuration filtering procedure is finally implemented to rule out the similar conformers with configurational deviations (measured in terms of RMSD) smaller than a cut-off value.

In total, 36 750 conformers are created. Compared to the original D–A molecule data size, on average it is equivalent to producing around 2–3 conformers for each D–A sample. More details relevant to the conformer set construction are given in the supplementary material. We employ the SchNet model (which performs the best on the original dataset) to examine the predictability of photophysical properties for TADF conformers.

Fig. 4 exhibits the SchNet predictions of the oscillator strengths and singlet–triplet splitting for the conformer set. The forecasting accuracies are satisfactory, especially for  $S_{1-f}$  and  $\Delta E_{ST}$  with the out-of-sample  $R^2$  being found to be 0.922 and 0.8502, respectively (Table 2). The accuracies are diminished for the higher excited state oscillator strengths, which is consistent with the model performances on the original set. It is interesting that the forecasting precisions of  $S_{1-f}$ ,  $S_{2-f}$  and  $S_{3-f}$  for the conformers are significantly improved compared to those for the original TADF (where a 20%–170% enhancement of  $R^2$  is observed), demonstrating the effectiveness of the enriched twisting information in promoting the predictability of the oscillator strengths. By further analysing the scattering plot of  $S_{1-f}$  in Fig. 4, we find that the SchNet prediction on the original set gives rise to a bunch of ‘true’ oscillators with the strengths being zero, while the predicted values are not, implying a reduced forecasting accuracy for molecules with a null  $f$  within the original D–A set. The phenomenon is

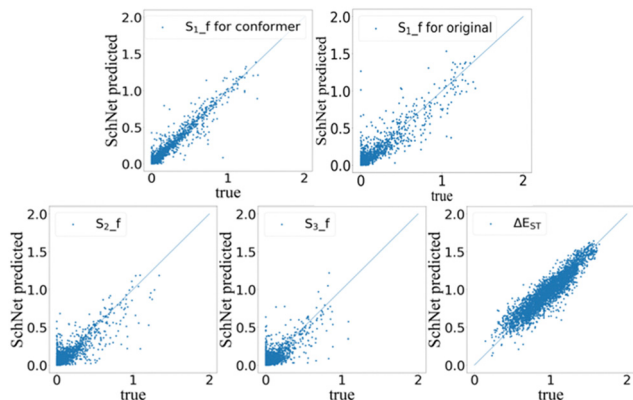


**Fig. 4** SchNet predictions of excited state properties for the TADF conformer test set. The true data indicate the high throughput calculations, and the blue line is the identity mapping. Note that  $\Delta E_{ST}$  is in the unit of eV, while  $f$  is dimensionless. The model cut-off radius is set to 5 Å. The upper right subfigure shows the SchNet prediction of  $S_{1-f}$  for the original set.

**Table 2** Test set predictive performances (with oscillator strengths and the energy gap being displayed) for SchNet when the model is applied on the original D–A dataset and the generated conformer dataset. The model cut-off is set to 20 Å for the original set and 5 Å for the conformer set

	SchNet for original set			SchNet for conformer set		
	$R^2$	RMSE	MAE	$R^2$	RMSE	MAE
$S_{1-f}$	0.7692	0.1309	0.0744	0.9220	0.0548	0.0296
$S_{2-f}$	0.2607	0.1490	0.0908	0.7018	0.0807	0.0476
$S_{3-f}$	0.2254	0.1089	0.0629	0.5484	0.0735	0.0457
$\Delta E_{ST}$	0.8877	0.0744	0.0566	0.8502	0.1013	0.0784

however suppressed for the prediction of conformers where SchNet can better discriminate the null and non-null  $f$ . No remarkable change is detected for the  $\Delta E_{ST}$  prediction accuracy between the conformer and original sets. Note that we adopt a 5 Å model cut-off for the conformer training, as it provides the best average performance for excited state properties compared to larger cut-offs.

Even though the predictive accuracies of the excited-state properties have been significantly improved with the conformer training, we notice that the understanding of the performance improvement is still limited. Considering that the enriched twisting information may help to better capture the first order oscillator strength (due to its direct relevance to the orbital overlap), similar improvement however does not occur for  $\Delta E_{ST}$ . Moreover, for  $S_{2-f}$  and  $S_{3-f}$ , the comprehension for the electronic structure of higher order excitations based on the model architecture would be complicated. We hereby claim that the article only deals with the predictability of excited-state properties, and leaves the interpretation of the ML inner mechanism for further explorations.

To the best of our knowledge, we have achieved a notably high prediction quality for the oscillator strength with the out-of-sample  $R^2$  approaching 0.92. The level is in significant contrast with the previous works, where  $R^2$  is reported in the limited range of 0.7–0.8,<sup>14,19</sup> and magnified predictive uncertainties can be encountered.<sup>13,20</sup> The current research reveals

that in addition to a sophisticated ML model, an extended torsional-angle profile between the donor and acceptor can be equally important for the accurate prediction of the transition dipoles.

In conclusion, this article has proposed a deep learning protocol to effectively forecast the electronic transition properties of delayed fluorescence molecules. Deep neural network, graph convolutional network, recurrent neural network, message passing neural network and SchNet models are employed to predict the transition energies, oscillator strengths and singlet–triplet splitting, which are critically relevant to the molecular design of TADF materials. Satisfactory performances are found, with  $R^2$  of the first oscillator strength above 0.7 and that of energy splitting above 0.85 being achieved, demonstrating the robustness of deep learning methods in describing the TADF mechanism. It is observed that the 1-dimensional representation (typified by RNN which uses the SMILES string) and 2-dimensional representation (typified by DNN which uses the circular fingerprint) can deliver comparable performances with the best performing 3-dimensional model (typified by SchNet, which uses atomic types and interatomic distances), implying the diversity of the neural network architectures that can be suitable for resolving the electronic transition. The investigation has provided a cost-effective ML framework for predictions of excited-state properties with a comparable accuracy to TDDFT calculations. Note that the limitations of TDDFT that we use to train our models may pose challenges in describing the real photophysical parameters, and further improvement of the ML predictive accuracy in regard to experimental properties would be subject to future research.

By developing the conformer database in terms of a stochastic search algorithm, we created a twisted D–A molecular set with extended torsional profiles based on the original TADF samples. High throughput TDDFT calculations are implemented to label the transition properties of more than 36 000 conformers. SchNet is employed to test the predictability of the oscillator strengths and the energy gap for the conformers. We found that the prediction qualities of  $S_{1-f}$ ,  $S_{2-f}$  and  $S_{3-f}$  are significantly improved compared to the original set with the  $R^2$  enhancement up to 170% being detected. The high level of precision (especially for the first oscillator) demonstrates that the enriched twisting information between the donor and acceptor can be important for the prediction of transition dipoles. The results could be indicative for the future work that a properly constructed database is equivalently essential to improve the material design efficiency for properties of interest.

## Conflicts of interest

There are no conflicts to declare.

## Acknowledgements

The work is supported by the Open Foundation of State Key Laboratory of Electronic Thin Films and Integrated Devices (No:

KFJJ202205) and Research Platform Foundation of Chengdu Polytechnic (No: 19KYPT01, No: 20KYTD07).

## Notes and references

- 1 H. Uoyama, K. Goushi, K. Shizu, H. Nomura and C. Adachi, *Nature*, 2012, **492**, 234–238.
- 2 M. Y. Wong and E. Zysman-Colman, *Adv. Mater.*, 2017, **29**, 1605444.
- 3 D. S. M. Ravinson and M. E. Thompson, *Mater. Horiz.*, 2020, **7**, 1210–1217.
- 4 S. P. Huang, Q. S. Zhang, Y. Shiota, T. Nakagawa, K. Kuwabara, K. Yoshizawa and C. Adachi, *J. Chem. Theory Comput.*, 2013, **9**, 3872–3877.
- 5 Z. Y. Yang, Z. Mao, Z. L. Xie, Y. Zhang, S. W. Liu, J. Zhao, J. R. Xu, Z. G. Chi and M. P. Aldred, *Chem. Soc. Rev.*, 2017, **46**, 915–1016.
- 6 X. Liang, Z. L. Tu and Y. X. Zheng, *Chem. – Eur. J.*, 2019, **25**, 5623–5642.
- 7 Z. Tan, Y. Li, Z. Y. Zhang, X. Wu, T. Penfold, W. M. Shi and S. Q. Yang, *ACS Omega*, 2022, **7**, 18179–18188.
- 8 H. Tanaka, S. Z. Katsuyuki, J. Y. Lee and C. Adachi, *J. Phys. Chem. C*, 2015, **119**, 2948–2955.
- 9 J. Y. Lee, *J. Mater. Chem. C*, 2015, **3**, 2175–2181.
- 10 D. R. Lee, S. H. Hwang, S. K. Jeon, C. W. Lee and J. Y. Lee, *Chem. Commun.*, 2015, **51**, 8105–8107.
- 11 T. Hatakeyama, K. Shiren, K. Nakajima, S. Nomura, S. Nakatsuka, K. Kinoshita, J. P. Ni, Y. Ono and T. Ikuta, *Adv. Mater.*, 2016, **28**, 2777–2781.
- 12 R. G. Bombarelli, J. A. Iparraguirre, T. D. Hirzel, D. Duvenaud, D. Maclaurin, M. A. B. Forsythe, H. S. Chae, M. Einzinger, D. G. Ha, T. Wu, G. Markopoulos, S. Jeon, H. Kang, H. Miyazaki, M. Numata, S. H. Kim, W. L. Huang, S. I. Hong, M. Baldo, R. P. Adams and A. A. Guzik, *Nat. Mater.*, 2016, **15**, 1120–1127.
- 13 C. Q. Lu, Q. Liu, Q. M. Sun, C. Y. Hsieh, S. Y. Zhang, L. Shi and C. K. Lee, *J. Phys. Chem. C*, 2020, **124**, 7048–7060.
- 14 B. Kang, C. Seok and J. Y. Lee, *J. Chem. Inf. Model.*, 2020, **60**, 5984–5994.
- 15 Z. Tan, Y. Li, W. M. Shi and S. Q. Yang, *J. Chem. Inf. Model.*, 2021, **61**, 3824–3834.
- 16 K. T. Schütt, H. E. Saucedo, P. J. Kindermans, A. Tkatchenko and K. R. Müller, *J. Chem. Phys.*, 2018, **148**, 241722.
- 17 S. Riniker and G. A. Landrum, *J. Chem. Inf. Model.*, 2015, **55**, 2562–2574.
- 18 P. Tosco, N. Stiefl and G. Landrum, *J. Cheminf.*, 2014, **6**, 37.
- 19 B. Kang, C. Seok and J. Y. Lee, *Bull. Korean Chem. Soc.*, 2022, **43**, 328.
- 20 S. Ye, W. Hu, X. Li, J. X. Zhang, K. Zhong, G. Z. Zhang, Y. Luo, S. Mukamel and J. Jiang, *Proc. Natl. Acad. Sci. U. S. A.*, 2019, **116**, 11612–11617.